

OPTIMIZATION OF FOUR-BUTTON BEAM POSITION MONITOR CONFIGURATION FOR SMALL-GAP VACUUM CHAMBERS

S. H. Kim
March 27, 1998

Summary - Induced charges on a four-button beam position monitor (BPM) system attached on a beam chamber of narrow rectangular cross sections are calculated as a 2-D electrostatic problem of image charges. The calculation shows that for a narrow chamber of width/height ($2w/2h$) $\gg 1$, over 90% of the induced charges are distributed within a distance of $2h$ from the charged beam position in the direction of the chamber width. Therefore, a four-button system with a button diameter of $(2 \sim 2.5)h$ and no button offset from the beam position is the most efficient configuration. The four-button BPMs used for 8-mm and 5-mm chambers in the APS have relatively low sensitivities because the button locations are outside the range where the induced charge densities are low and the button diameters are less than $2h$. Using derived formulae, button sensitivities and beam position coefficients are calculated for the buttons of the most efficient case and of the 8-mm and 5-mm chambers. The formulae may be used to validate the method of computer modeling for BPM buttons on a beam chamber of an arbitrary cross section.

1. INTRODUCTION

For a point charge λ moving with a constant velocity v in the z direction, the electric field in the laboratory frame derived from the Lienard-Wiechert potential is given by [1]

$$E = \frac{\lambda}{4\pi\epsilon_0 r^2} \frac{1 - \beta^2}{(1 - \beta^2 \sin^2 \theta)^{3/2}}, \quad (1)$$

where $\beta = v/c$, c is the velocity of light, r is the distance from the position of the charge to an observation point, and θ is the angle between the z -direction and the observation point at the position of the charge. By integrating $E \cdot 2\pi r^2 \sin \theta d\theta$, the electric flux between two given angles can be calculated. For $\gamma = 1/\sqrt{1 - \beta^2} \gg 1$, a fraction f of the total electric flux is concentrated within an angle of $\pm 1/\gamma (f / \sqrt{1 - f^2})$ of the transverse plane to the z direction. For example, for $\gamma = 2 \times 10^3$, 90% of the total electric flux is concentrated within an angle of ± 1.04 mrad. In this note, therefore, calculations of induced charges on button-type pickups for a BPM system are considered as a 2-D electrostatic problem.

2. IMAGE CHARGES

Assuming that the width of the beam chamber in Fig. 1 is much larger than the height ($w \gg h$), the induced charges are calculated by the methods of image charge. The beam chamber is also assumed to have a high electric conductivity and is grounded. Then the vertical positions of the positive and negative image charges of a charge λ at (x_0, y_0) are given by

$$\begin{aligned}
& +\lambda \text{ at } y = 2m(a + b) + y_o = 4mh + y_o, & (m = -\infty, 0, \infty) \\
& \text{and } -\lambda \text{ at } y = 2a + 2m(a + b) + y_o = 2a + 4mh + y_o & (m = -\infty, 0, \infty) \\
& \text{with } a = h - y_o \text{ and } b = h + y_o.
\end{aligned} \tag{2}$$

For ease of calculation the vertical position for $(-\lambda)$ is shifted by $2h$ so that $y' = y - 2h = 4mh - y_o$. (In the 3-D geometry the charge λ is a line-charge density along the z direction.)

Then the electrostatic potential distribution $\Phi(x, y)$ within the chamber may be calculated from [2]

$$\Phi(x, y) = \frac{-\lambda}{2\pi\epsilon_0} \ln \frac{\prod_{m=-\infty}^{\infty} |z - z_m|}{\prod_{m=-\infty}^{\infty} |z' - z'_m|} = \frac{-\lambda}{2\pi\epsilon_0} \ln \frac{|z - z_o| \prod_{m=1}^{\infty} |(z - z_m)(z - z_{-m})|}{|z' - z'_o| \prod_{m=1}^{\infty} |(z' - z'_m)(z' - z'_{-m})|}, \tag{3}$$

where ϵ_0 is the permittivity constant, $z = x + i y$, $z' = x + i y'$, $z_{\pm m} = x_o + i (\pm 4mh + y_o)$, and $z'_{\pm m} = x_o + i y' = x_o + i (\pm 4mh - y_o)$. Using the relation

$$\sin z = z \prod_{n=1}^{\infty} \left[1 - \left(\frac{z}{n\pi} \right)^2 \right],$$

Eq. (3) may be simplified to a closed form

$$\begin{aligned}
\Phi(x, y) &= \frac{-\lambda}{2\pi\epsilon_0} \operatorname{Re} \left\{ \ln \frac{\sin \pi \left(\frac{z - x_o - iy_o}{4hi} \right)}{\sin \pi \left(\frac{z' - x_o + iy_o}{4hi} \right)} \right\} \\
&= \frac{-\lambda}{4\pi\epsilon_0} \ln \frac{\cosh \pi \frac{x - x_o}{2h} - \cos \pi \frac{y - y_o}{2h}}{\cosh \pi \frac{x - x_o}{2h} - \cos \pi \frac{y' + y_o}{2h}} = \frac{-\lambda}{4\pi\epsilon_0} \ln \frac{\cosh \pi \frac{x - x_o}{2h} - \cos \pi \frac{y - y_o}{2h}}{\cosh \pi \frac{x - x_o}{2h} + \cos \pi \frac{y + y_o}{2h}},
\end{aligned} \tag{4}$$

where y' is shifted back to $y + 2h$ in the final expression.

The induced charge densities per x/h in the top and bottom surfaces of the chamber, σ_t and σ_b , are calculated from $[-\epsilon_0 d\Phi/dy]_{y=\pm h}$:

$$\begin{aligned}
\sigma_t &= -\frac{\lambda}{4} \frac{\cos p y_o}{\cosh p(x - x_o) - \sin p y_o}, \\
\sigma_b &= -\frac{\lambda}{4} \frac{\cos p y_o}{\cosh p(x - x_o) + \sin p y_o}.
\end{aligned} \tag{5}$$

Here $p = \pi/2$ and by setting $h = 1$ the coordinate system is normalized to the half height of the chamber. (The normalization is used for Eqs. (5) - (10).) By adding up the induced charges in

the top and bottom surfaces in Eq. (5), the total induced charge, which should be proportional to the sum signal for a typical four-button BPM system of Fig. 1, is given by

$$\begin{aligned} Q_s &= Q_s(x_2) - Q_s(x_1) = \int_{x_1}^{x_2} (\sigma_t + \sigma_b) dx + \int_{-x_2}^{-x_1} (\sigma_t + \sigma_b) dx \\ &= -\lambda \frac{1}{2} \int_{x_1}^{x_2} \left\{ \frac{\cos py_o \cosh p(x - x_o)}{\cosh^2 p(x - x_o) - \sin^2 py_o} + \frac{\cos py_o \cosh p(x + x_o)}{\cosh^2 p(x + x_o) - \sin^2 py_o} \right\} dx. \end{aligned} \quad (6)$$

The induced charges proportional to the signals for the vertical and horizontal positions of the charged beam, Q_y and Q_x , may be calculated from Eq. (5):

$$\begin{aligned} Q_y &= Q_y(x_2) - Q_y(x_1) = \int_{x_1}^{x_2} (\sigma_t - \sigma_b) dx + \int_{-x_2}^{-x_1} (\sigma_t - \sigma_b) dx \\ &= -\lambda \frac{1}{2} \int_{x_1}^{x_2} \left\{ \frac{\sin py_o \cos py_o}{\cosh^2 p(x - x_o) - \sin^2 py_o} + \frac{\sin py_o \cos py_o}{\cosh^2 p(x + x_o) - \sin^2 py_o} \right\} dx, \end{aligned} \quad (7)$$

$$\begin{aligned} Q_x &= Q_x(x_2) - Q_x(x_1) = \int_{x_1}^{x_2} (\sigma_t + \sigma_b) dx - \int_{-x_2}^{-x_1} (\sigma_t + \sigma_b) dx \\ &= -\lambda \frac{1}{2} \int_{x_1}^{x_2} \left\{ \frac{\cos py_o \cosh p(x - x_o)}{\cosh^2 p(x - x_o) - \sin^2 py_o} - \frac{\cos py_o \cosh p(x + x_o)}{\cosh^2 p(x + x_o) - \sin^2 py_o} \right\} dx. \end{aligned} \quad (8)$$

Here Q_y and Q_x are the differences in the induced charges between the top and bottom, and right and left buttons, respectively. As one expects from beam position measurements, Q_y is an odd function in y_o and even in x_o , and Q_x is the opposite. After Taylor expansions up to the third order in the charged beam position (x_o, y_o) , indefinite integrals of Eqs. (6) - (8) are given by

$$\begin{aligned} \frac{Q_s(x)}{-\lambda} &= \frac{1}{p} \tan^{-1}[\sinh px] + (y_o^2 - x_o^2) \frac{p \sinh px}{2 \cosh^2 px} + y_o^2 x_o^2 \frac{p^3}{4} \left(\frac{\sinh px}{\cosh^2 px} - \frac{6 \sinh px}{\cosh^4 px} \right), \\ \frac{Q_y(x)}{-\lambda} &= y_o [\tanh px + x_o^2 p^2 \frac{-\sinh px}{\cosh^3 px}] + y_o^3 [p^2 \frac{\sinh px}{3 \cosh^3 px} + x_o^2 p^4 (\frac{2 \sinh px}{3 \cosh^3 px} - \frac{2 \sinh px}{\cosh^5 px})], \\ \frac{Q_x(x)}{-\lambda} &= x_o [-\sec h(px) + y_o^2 p^2 \{ \frac{1}{2} \sec h(px) - \sec h^3(px) \}] + x_o^3 [\frac{p^2}{6} \{ 2 \sec h^3(px) \\ &\quad - \sec h(px) \} + y_o^2 p^4 \{ 2 \sec h^5(px) - \frac{5}{3} \sec h^3(px) + \frac{1}{12} \sec h(px) \}]. \end{aligned} \quad (9)$$

To the first order in y_o/h and x_o/h , calculations of the induced charges from $x_1 = 0$ to $x_2 = \infty$ in Eq. (9) give $Q_y = -\lambda y_o/h$, $Q_x = -\lambda x_o/h$, and the total induced charge $Q_s = -\lambda$ as expected. The above three equations will be used to calculate the button sensitivity and coefficients for y_o/h and x_o/h . The derivatives of $Q_s(x)$, $Q_y(x)$, and $Q_x(x)$ with respect to x/h

may be called “the effective induced charge densities for the sum, vertical, and horizontal signals.” Their first terms are

$$\begin{aligned} dQ_s(x)/dx &= -\lambda \sec h(px), \\ dQ_y(x)/dx &= -y_0 p \lambda \sec h^2(px), \\ dQ_x(x)/dx &= -x_0 p \lambda \sinh(px) \sec h^2(px). \end{aligned} \quad (10)$$

Equation (10) and the first terms of Eq. (9) are plotted in Fig. 2. Here the induced charges and the respective densities for Q_s , Q_y , and Q_x are denoted as sum, vert, and horz in the figure legend, respectively, with units of $-\lambda$, $-\lambda y_0/h$, and $-\lambda x_0/h$. (The units of the charge densities for Q_s , Q_y , and Q_x should be $-\lambda/h$, $-\lambda y_0/h^2$, and $-\lambda x_0/h^2$ if plotted in x instead of x/h .) For small buttons (e.g. $x/h < 0.5$), when the beam is located near the origin, the horizontal beam displacement is not as sensitive to changes in the distances between the beam and the buttons as the vertical beam displacement. This makes the density distribution for Q_x broad with the peak near $x/h = 0.6$. The density for Q_y , on the other hand, has its peak at $x/h = 0$. This implies that, when the measurements of vertical displacements are critical for a beam chamber of small height, the location of the buttons should include the range of small x/h . For buttons located in the range of $x = 0 - 2h$ with button diameter of $2h$, for example, over 94%, 99%, and 91% of the available sensitivities for sum, vert, and horz can be registered on the buttons. Therefore, any buttons located more than $2h$ (one chamber height) from the beam position in the horizontal direction would be very inefficient.

Shown in Fig. 3 are 3-D plots and their contours for Q_s , Q_y , and Q_x . The negative position of x_1 is possible by rotating the four-button system with respect to the vertically symmetrical axis. For $x_1 = 0$ and a button diameter d larger than $2h$, it is seen that Q_s , Q_y , and Q_x do saturate as already expected from Fig. 2. When the buttons are extended to both sides of the x -axis by rotating the four-button system and the diameter is larger than $4h$, the values of Q_s and Q_y increase by a factor of 2 because most parts of the buttons are still located within $x/h < 2$ where the charge densities are high. On the other hand, Q_x decreases because the charge density for Q_x in Eq. (10) is asymmetric with respect to x . Therefore, a four-button system with a button diameter of approximately $(2 \sim 2.5)h$ and a button offset of $x_1 = 0$ would collect nearly all the induced charges and be the most efficient.

3. BUTTON SENSITIVITIES

It is seen from Figs. 2 and 3 that button sensitivities of over 90% of the induced charges can be obtained for a button diameter of $(2 \sim 2.5)h$ and a button offset of $x_1 = 0$. With $x_1 = 0$ and $d = 2h$, where the button diameter d is $(x_2 - x_1)h$, Q_s , Q_y , Q_x , and their normalized values to Q_s are calculated from Eqs. (6) - (8). The results give an optimized BPM configuration and are plotted in Fig. 4 as functions of the normalized beam position (y_0/h , x_0/h). The button sensitivities and coefficients for y_0/h and x_0/h for the optimized configuration are calculated from Eq. (9).

Optimized configuration:

$$\begin{aligned} Q_s &= 0.945[1.0 + 0.07143 \{(y_0/h)^2 - (x_0/h)^2\} + 0.0842 (x_0/h)^2 (y_0/h)^2], \\ Q_y &= 0.9963[\{1.0 - 0.01836 (x_0/h)^2\}(y_0/h) + \{0.00612 + 0.0295 (x_0/h)^2\}(y_0/h)^3], \end{aligned}$$

$$\begin{aligned}
Q_x &= 0.9137[\{1.0 + 1.4649 (y_o/h)^2\}(x_o/h) - \{0.4883 + 2.7354 (y_o/h)^2\}(x_o/h)^3], \\
Q_y/Q_s &= 1.0542[\{1 + 0.0531 (x_o/h)^2\}(y_o/h) - \{0.0653 + 0.0631 (x_o/h)^2\}(y_o/h)^3], \\
Q_x/Q_s &= 0.9669[\{1 + 1.3935 (y_o/h)^2\}(x_o/h) - \{0.4169 + 2.6159 (y_o/h)^2\}(x_o/h)^3]. \quad (11)
\end{aligned}$$

It is seen from Fig. 4(a) and Eq. (11) that the vertical signal Q_y and Q_y/Q_s within $\pm 0.7y_o/h$ have excellent linearity in y_o/h and x_o/h . This is particularly important since vertical measurements are generally critical in a small chamber height. The horizontal signals Q_x and Q_x/Q_s , on the other hand, are less linear compared to those for the vertical as seen from Fig. 4(b) and the coefficients of y_o/h and x_o/h in Eq. (11).

In the APS storage ring, beam chambers with relatively small chamber heights are used for the insertion devices (IDs) in the straight sections. Several four-button BPMs with button diameters of 4 mm and button-center separations of 9.65 mm have been installed for chamber heights of 8 mm ($h = 4$ mm, $x_1 = 0.7075h$, $x_2 = 1.7075h$, diameter = $1.0h$) and 5 mm ($h = 2.5$ mm, $x_1 = 1.132h$, $x_2 = 2.732h$, diameter = $1.6h$). One can see from Fig. 2 that these buttons are located at relatively inefficient positions compared to an ideal case of $x_1 = 0$ and $x_2 = 2h$. The button sensitivities and y_o and x_o coefficients for the two chambers are calculated from Eq. (9).

APS ID chamber ($2h = 8$ mm):

$$\begin{aligned}
Q_s &= 0.3178[1.0 + 0.0529 \{x_o^2 - y_o^2\} + 0.00778 x_o^2 y_o^2], \\
Q_y &= 0.0465[\{1.0 + 0.2199 x_o^2\} y_o + \{-0.0733 + 0.00228 x_o^2\} y_o^3], \\
Q_x &= 0.1144[\{1.0 - 0.00738 y_o^2\} x_o + \{0.00246 + 0.00827 y_o^2\} x_o^3], \\
Q_y/Q_s &= 0.1464 [\{1 + 0.1669 x_o^2\} y_o + \{-0.2033 + 0.00502 x_o^2\} y_o^3], \\
Q_x/Q_s &= 0.360 [\{1 + 0.0456 y_o^2\} x_o + \{-0.5049 + 0.00229 y_o^2\} x_o^3]. \quad (12)
\end{aligned}$$

The smallest aperture APS chamber ($2h = 5$ mm):

$$\begin{aligned}
Q_s &= 0.1957[1.0 + 0.1817 \{x_o^2 - y_o^2\} - 0.0104 x_o^2 y_o^2], \\
Q_y &= 0.02205[\{1.0 + 0.7246 x_o^2\} y_o - \{0.2415 + 0.1285 x_o^2\} y_o^3], \\
Q_x &= 0.1205[\{1.0 - 0.1509 y_o^2\} x_o + \{0.0503 + 0.0136 y_o^2\} x_o^3], \\
Q_y/Q_s &= 0.1127 [\{1 + 0.5429 x_o^2\} y_o - \{0.0598 + 0.00858 x_o^2\} y_o^3], \\
Q_x/Q_s &= 0.6156 [\{1 + 0.0308 y_o^2\} x_o - \{0.1314 + 0.0146 y_o^2\} x_o^3]. \quad (13)
\end{aligned}$$

The button sensitivities for the above two chambers are plotted in Figs. 5 and 6. As seen from the figures and Eqs. (12) and (13), the most critical signals Q_y for 8-mm and 5-mm chambers are only 0.045 and 0.022 of the unit $-\lambda y_o/h$. Compared to Q_y , the horizontal signals Q_x are

over 0.11 of the unit $-\lambda x_o/h$ for both chambers. Even if the normalized signals are not too small (because of the small values of Q_s), one should expect that the noise/signal ratios for Q_y/Q_s and Q_x/Q_s in Eqs. (12) and (13) are relatively large compared to those in Eq. (11).

ACKNOWLEDGEMENTS

The author appreciates G. Decker for his numerous suggestions for this work.

REFERENCES

- [1] See, for example, W. K. H. Panofsky and M. Phillips, *Classical Electricity and Magnetism* (Addison-Wesley, Cambridge, MA, 1955) p. 290.
- [2] See, for example, D. A. Edwards and M. J. Syphers, *An Introduction to the Physics of High Energy Accelerators* (John Wiley & Sons, Inc, New York, 1993) p. 179.

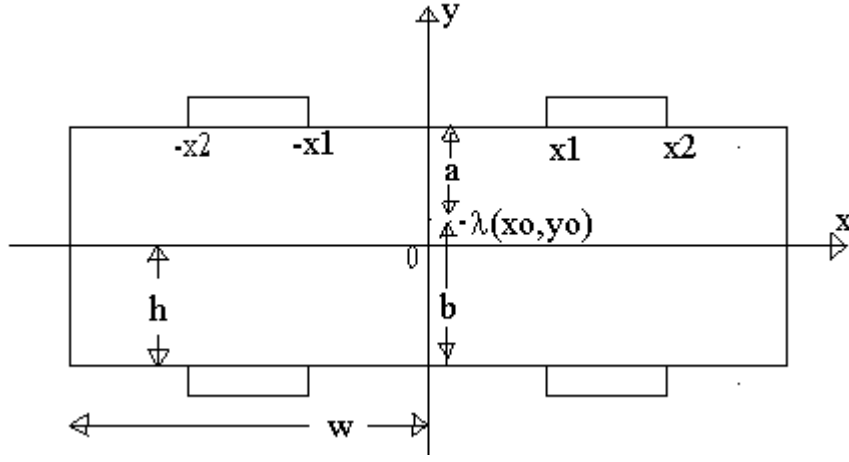


Fig. 1. Cross section of a beam chamber with a height of h and width of w . The chamber is assumed to be grounded. The charge λ at (x_0, y_0) is the line-charge density in the 3-D geometry. The diameter of the four buttons for the BPM system is $(x_2 - x_1)$, and $b = h + y_0$, $a = h - y_0$.

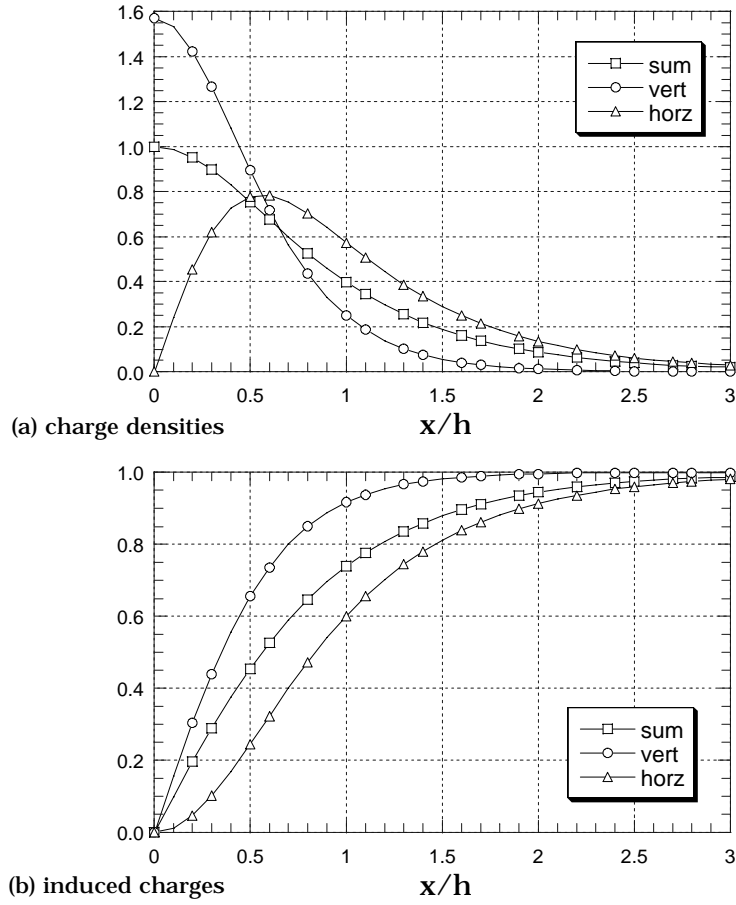


Fig. 2. (a) Induced charge densities of Eq. (10) and (b) induced charges integrated from 0 to x/h . The induced charges and densities corresponding to Q_s , Q_y , and Q_x in Eq. (9) are denoted as sum, vert, and horz in the legends, respectively, with units of $-\lambda$, $-\lambda y_0/h$, and $-\lambda x_0/h$.

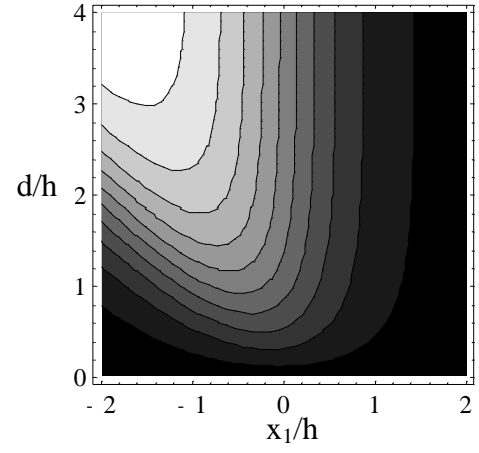
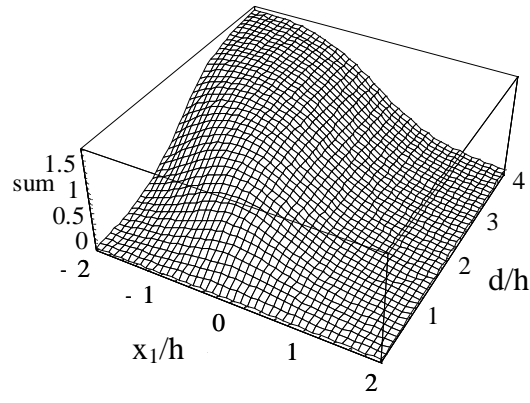
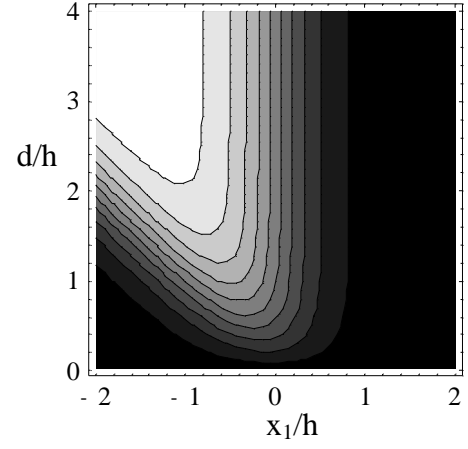
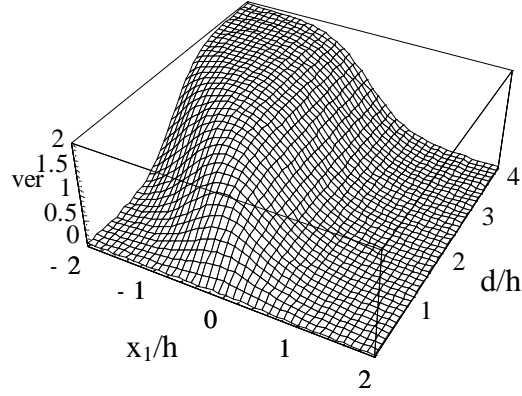
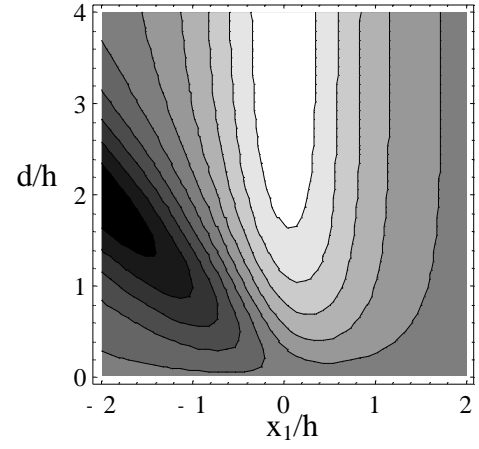
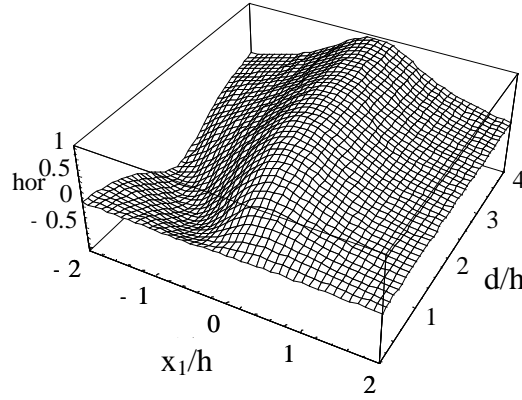
(a) Q_s (b) Q_y (c) Q_x 

Fig. 3. 3-D plots of the induced charges for Q_s , Q_y , and Q_x of Eq. (6) - (8) as functions of normalized button offset x_1/h and button diameter d/h on the left side, and their contour plots on the right side. The respective units for Q_s , Q_y , and Q_x are $-\lambda$, $-\lambda y_o/h$, and $-\lambda x_o/h$.

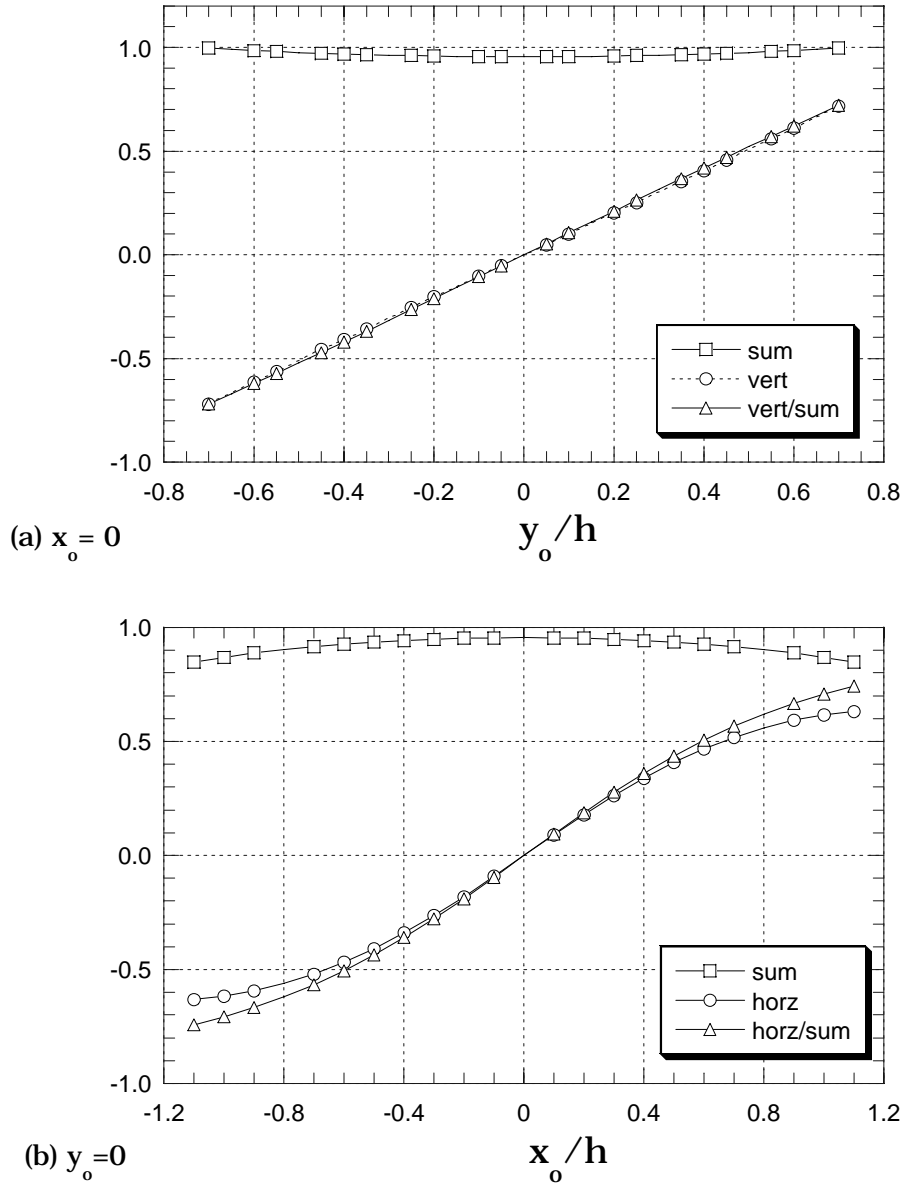


Fig. 4. For the optimized BPM configuration, normalized button positions of $x_1/h = 0$ and $x_2/h = 2$ (normalized diameter $d/h = 2$), variations (a) Q_s , Q_y , and Q_y/Q_s are plotted as a function of normalized vertical beam position y_o/h for $x_o = 0$, and (b) Q_s , Q_x , and Q_x/Q_s as a function of normalized horizontal beam position x_o/h for $y_o = 0$. Here Q_s , Q_y , and Q_x are denoted as sum, vert, and horz and their respective units are $-\lambda$, $-\lambda y_o/h$, and $-\lambda x_o/h$. Note that for small values of x_o/h and y_o/h , Q_s , Q_y , and Q_x are over 0.9 of their respective units.

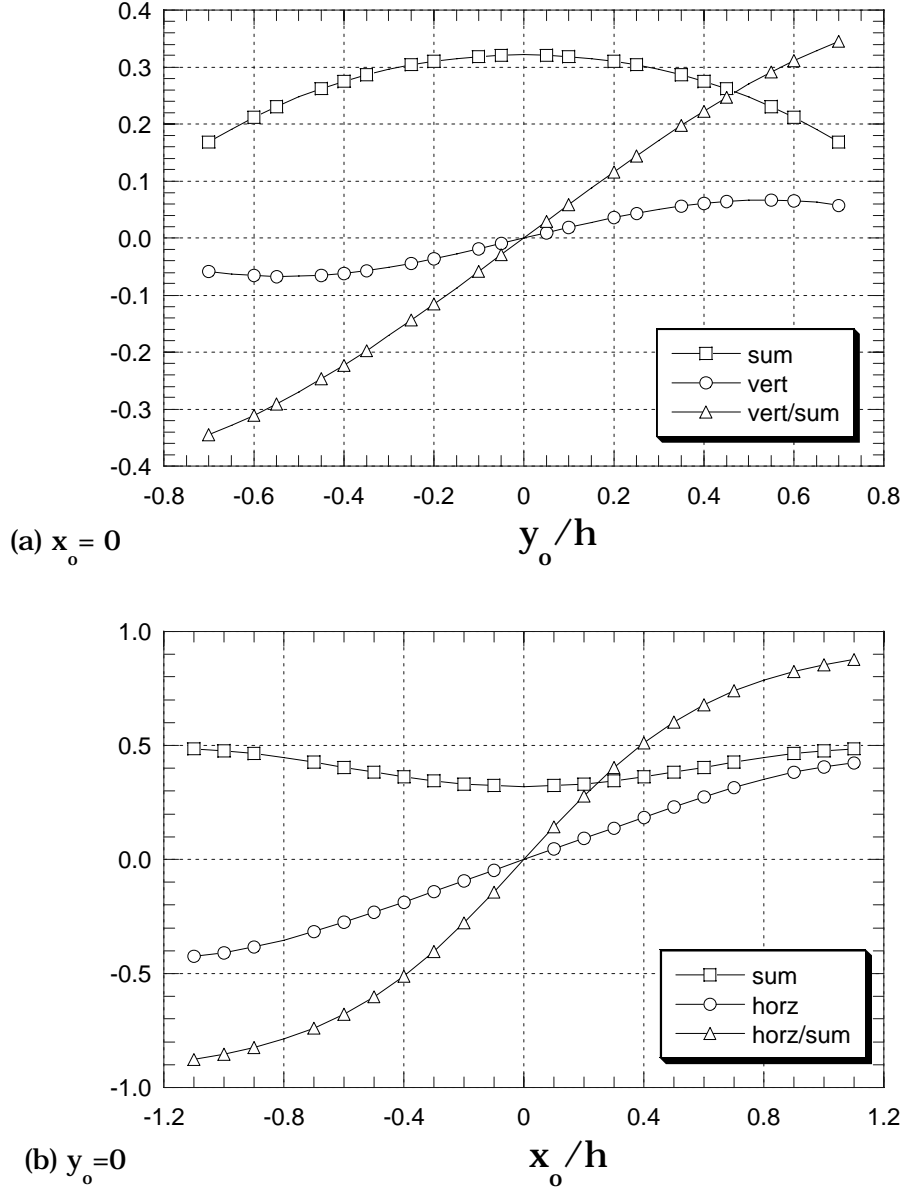


Fig. 5. For an 8-mm chamber ($h = 4$ mm) similar to an APS ID chamber with normalized button positions of $x_1/h = 0.7075$ and $x_2/h = 1.7075$ and button diameter $(x_2 - x_1)h = h$, variations (a) Q_s , Q_y , and Q_y/Q_s as a function of y_o/h for $x_o = 0$, and (b) Q_s , Q_x , and Q_x/Q_s as a function of x_o/h for $y_o = 0$. Here Q_s , Q_y , and Q_x are denoted as sum, vert, and horz and their respective units are $-\lambda$, $-\lambda y_o/h$, and $-\lambda x_o/h$. Note that for small values of x_o/h and y_o/h , Q_s , Q_y , and Q_x are only 0.32, 0.05, and 0.12 of their respective units and the button system is inefficient.

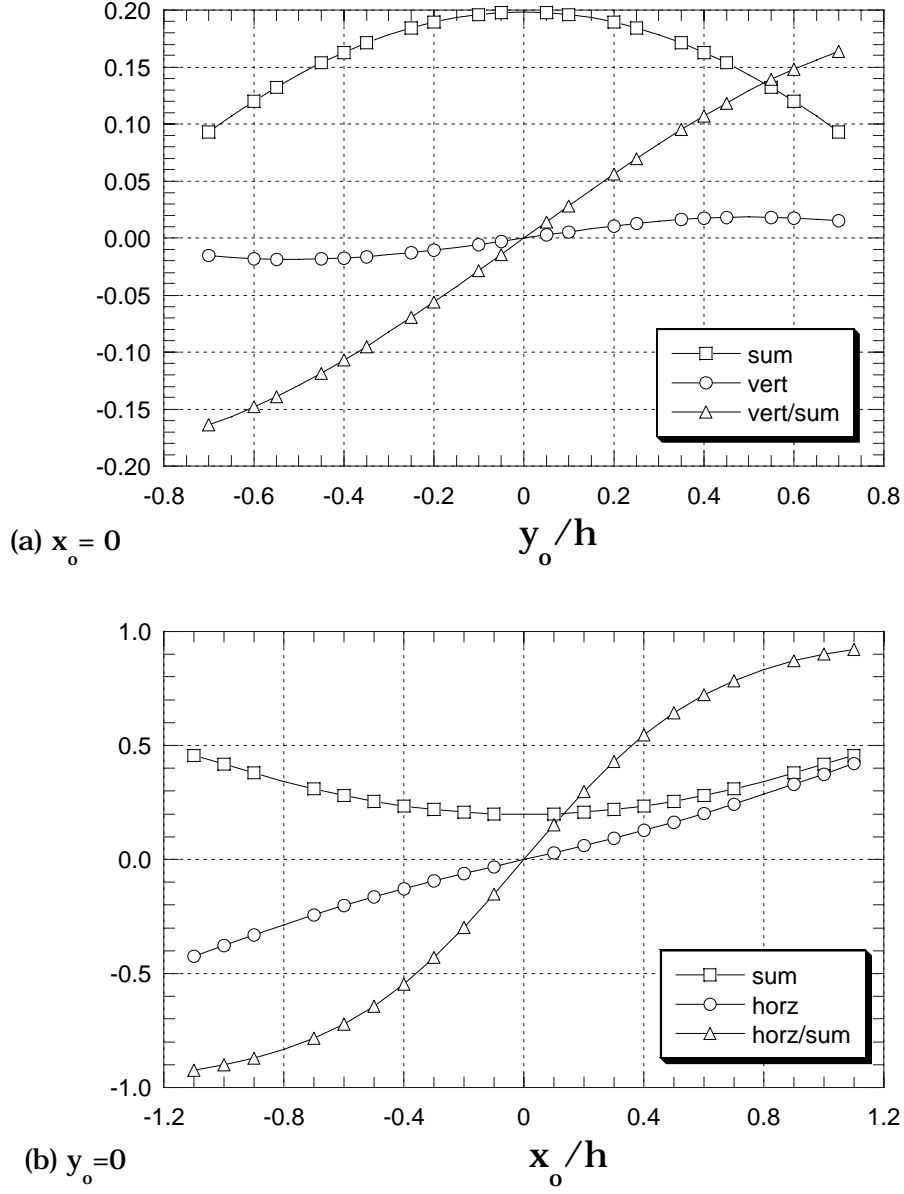


Fig. 6. For a 5-mm chamber ($h = 2.5$ mm) similar to the smallest aperture APS chamber with normalized button positions of $x_1/h = 1.132$ and $x_2/h = 2.732$ and button diameter $(x_2 - x_1)h = 1.6 h$, variations (a) Q_s , Q_y , and Q_y/Q_s as a function of y_o/h for $x_o = 0$, and (b) Q_s , Q_x , and Q_x/Q_s as a function of x_o/h for $y_o = 0$. Here Q_s , Q_y , and Q_x are denoted as sum, vert, and horz and their respective units are $-\lambda$, $-\lambda y_o/h$, and $-\lambda x_o/h$. Note that for small values of x_o/h and y_o/h , Q_s , Q_y , and Q_x are only 0.2, 0.022, and 0.11 of their respective units and the button system is very inefficient.